Mon. Not. R. Astron. Soc. **000**, 1–14 (0000) Printed 5 February 2008 (MN LATEX style file v2.2)

The Bright End of the Luminosity Function of Red Sequence Galaxies

Yeong-Shang Loh[1,2,3⋆] and Michael A. Strauss[1]
[1]*Princeton University Observatory, Princeton, NJ 08544*
[2]*Department of Physics, Princeton University, Princeton, NJ 08544*
[3]*Center for Astrophysics and Space Astronomy, University of Colorado, Boulder, CO 80309*

5 February 2008

ABSTRACT
We study the bright end of the luminosity distribution of galaxies in fields with Luminous Red Galaxies (LRG) from the Sloan Digital Sky Survey (SDSS). Using $2099\,\mathrm{deg}^2$ of SDSS imaging data, we search for luminous ($\gtrsim L^*$) early-type galaxies within $1.0\,h^{-1}\,\mathrm{Mpc}$ of a volume-limited sample of $12,608$ spectroscopic LRG in the redshift range $0.12 < z < 0.38$. Most of these objects lie in rich environments, with the LRG being the brightest object within $1.0\,h^{-1}\,\mathrm{Mpc}$. The luminosity gap, M_{12}, between the first and second-rank galaxies within $1.0\,h^{-1}\,\mathrm{Mpc}$ is large (~ 0.8 mag), substantially larger than can be explained with an exponentially decaying luminosity function of galaxies. The brightest member is less luminous (by 0.1 – 0.2 mag), and shows a larger gap in LRG selected groups than in cluster-like environments. The large luminosity gap shows little evolution with redshift to $z = 0.4$, ruling out the scenario that these LRG selected brightest cluster or group galaxies grow by recent cannibalism of cluster members.

Key words: methods: statistical – galaxies: elliptical and lenticular, cD – galaxies: evolution – galaxies: clusters: general

1 INTRODUCTION

The bright end of the galaxy luminosity function is still not completely characterized. While uncertainties about surface brightness completeness is an issue at the faint end (Dalcanton 1998), the limiting factor at the bright end is often small number statistics. Early studies of the bright end of the galaxy luminosity function focused on high density regions, often in the richest clusters of galaxies. The galaxy number counts drop sharply around the characteristic luminosity (L_*)[1] so fitting functions used to describe the luminosity function (expressed in magnitude) have a decaying bright end – Abell (1965) used a power-law, Hubble (1936) a Gaussian, while Schechter (1976) a double exponential – all of which by construction predict a small number at the brightest extreme. Hence, the occurrence of even a single galaxy at large luminosity ($\gtrsim 10\,L_*$) would seem improbable. However, early studies of composite cluster luminosity functions show an ubiquitous bright end "hump" populated by the brightest members. For example, in his seminal paper, Schechter (1976) found that the Gamma distribution (in luminosity) provides an excellent fit to the composite galaxy luminosity function of 13 massive clusters of galaxies in the local universe when the brightest galaxy of each cluster is excluded from the fit. This result has been reproduced by many investigators (Colless 1989; Lugger 1989; Valotto et al. 1997; Lumsden et al. 1997; Trentham 1998; Garilli et al. 1999; Paolillo et al. 2001; Yagi et al. 2002; Goto et al. 2003).

With the advent of wide-angle redshift surveys, the field galaxy luminosity function has been increasingly well measured (Loveday et al. 1992; Norberg et al. 2002; Blanton et al. 2003a). In these data, the bright hump seen in the galaxy luminosity function derived from rich clusters is either absent or not as pronounce. When careful correction for Eddington (1913) bias due to photometric scatter is included in the likelihood fit to the luminosity function, the extreme plunging in number counts predicted from a double exponential, is confirmed both locally (Blanton et al. 2003a) and up to $z \sim 0.4$ (Loh 2003). This prompted Schechter (2002) among others to conclude that the bright end shape of the galaxy luminosity function is universal– it cuts off exponentially in luminosity, matching the analytical mass function in the Press & Schechter (1974) formalism – lending credence to the mass upper bound calculations of Rees & Ostriker (1977).

In addition to their extreme luminosities, brightest galaxies in clusters are often distinguished as having disturbed morphologies and extended low surface brightness stellar halos. Ostriker and collaborators (Ostriker & Tremaine 1975; Ostriker & Hausman 1977; Hausman & Ostriker 1978, but see also Richstone 1975, 1976; White 1976; Binney 1977; Gunn & Tinsley 1977) have proposed

⋆ E-mail: yeongloh@colorado.edu
[1] In this paper, we use M^* (the characteristic absolute magnitude of the knee of the luminosity function) and L_* (the corresponding luminosity) interchangeably.

that these properties are a consequence of being centrally located in high density environments. Indeed, the majority of such objects are found in high density environments, and only rarely does the luminosity function of moderately rich groups (cf. Geller & Postman 1983) exhibit a hump. Hence, accretion via tidal stripping, and merger activity via dynamical frinction in rich environments would seem to be responsible for their growth. However, careful numerical and analytical modeling of cluster environments (Merritt 1984, 1985; Tremaine 1990) suggest that the luminosities of Brightest Cluster Galaxies (BCGs) increase only slightly in a Hubble time, as the large velocity dispersions of the galaxy in these rich clusters makes the proposed cannibalistic scenario inefficient. Cannibalism, if it were to operate solely at the present epoch, is insufficient to explain the observed magnitude difference Δm_{12} (hereafter the *dominance*) between the BCG and the second brightest galaxy in rich clusters. Recent state of the art numerical simulations of massive clusters in a cosmological context (Gao et al. 2004; Athanassoula, Garijo & Garcia Gómez 2001; Dubinsky 1998; see also earlier work by West 1994; Bode et al. 1994) suggest that BCG dominance is driven primary by cosmological infall, and it thus develops as the clusters themselves form.

In this paper, we use data from the Sloan Digital Sky Survey (SDSS; York et al. 2000) to examine the dependence of the luminosity difference between the BCG and the second-ranked member on environment and redshift, to test these various evolutionary scenarios. Rather than selecting galaxies in *a priori* chosen dense environments, we sample the field for the most luminous red galaxies (i.e., those with the largest stellar masses) at each cosmological epoch, using a selection algorithm based on colors and apparent magnitudes of a passively evolving old stellar population.

Specifically, this paper investigates the bright end behavior of the luminosity function in regions that host at least one spectroscopic Luminous Red Galaxy (hereafter LRG; Eisenstein et al. 2001) from the SDSS. All high-density regions contain one or more LRGs but LRGs also sample lower density environments (e.g. Loh et al. 2005b; Eisenstein et al. 2005), including objects without companions to the flux limit of the SDSS within $\sim 1.0\,h^{-1}\,\mathrm{Mpc}$. This work complements older studies using samples selected by galaxy overdensities (Tremaine & Richstone 1977; Geller & Postman 1983; Bhavsar & Barrow 1985) and can test the dominance-overdensity hypothesis. It also has a potentially cleaner interpretation, as overdensity-selected samples are often subjected to bias from projection effects, and by the so-called *selection* effect (Scott 1957) when comparing samples over a range of redshift.

The outline of the paper is as follows: In the next section, we describe the sample used in our analysis. We describe the statistical tests used in section 3. In section 4, we outline in detail the implementation of our analysis, including a description of the various subsamples used. In section 5, we present our results and give caveats that need to be taken into account for robust interpretation in section 6. Finally, in section 7, we summarize our key conclusions. Throughout this paper, $h = H_0/100\ \mathrm{km\ s^{-1}\ Mpc^{-1}}$ and we adopt the concordance $\Omega_m = 0.3, \Omega_\Lambda = 0.7$ cosmology.

2 SAMPLE

2.1 The SDSS Survey

The SDSS will eventually image a quarter of the Celestial Sphere and obtain spectra of approximately 1 million sources. The 5 band (*ugriz*, Fukugita et al. 1996) imaging is done simultaneously during photometric conditions (Hogg et al. 2001) using a specially designed wide-field camera (Gunn et al. 1998) in drift-scanning mode. The imaging data are processed by automated pipelines that detect and measure photometric properties (Lupton et al. 2001), and astrometrically and photometrically calibrated the data (Pier et al. 2003; Smith et al. 2002; Ivezic et al. 2004). From the imaging survey, sources are selected for spectroscopy using a 640 fiber spectrograph mounted on the same telescope. To date, SDSS has had four major public data releases: the Early Data Release (EDR; Stoughton et al. 2002), Data Release One (DR1; Abazajian et al. 2003), Data Release Two (DR2; Abazajian et al. 2004) and Data Release Three (DR3; Abazajian et al. 2005). The data used for this paper are drawn from DR1.

2.2 Luminous Red Galaxy Sample

The LRG sample (Eisenstein et al. 2001) is a set of intrinsically red and luminous ($\gtrsim 3L^*$) galaxies targeted spectroscopically by SDSS to create a large-volume galaxy survey at moderate number density, out to $z \approx 0.5$. The full LRG sample comprises $\sim 12\%$ of all SDSS galaxy spectroscopic targets (Strauss et al. 2002). Here, we use those LRGs selected by "Cut I" – galaxies that lie on the linear locus of $g - r$ and $r - i$ color space – to give an approximately volume-limited sample to $r_{\mathrm{lim}} = 19.2$ at $z < 0.38$.

The luminosities and colors of giant elliptical galaxies are observed to evolve slowly, and aside from the outer stellar envelope of BCGs and cDs, the stars in these galaxies are believed to have formed at high redshift, e.g. $z > 2$ (Gunn & Oke 1975; Ellis et al. 1997; Aragón-Salamanca, Baugh & Kauffmann 1998; Stanford, Eisenhardt & Dickinson 1998; van Dokkum et al. 1998; Burke, Collins & Mann 2000). The LRG target selection, described in detail by Eisenstein et al. (2001), tunes its selection criteria (based on the uniform SDSS photometry) to match the luminosity and color of a passively evolving old stellar population. The K-corrections as a function of redshift are such that the contamination from intrinsically blue and low-luminosity objects is essentially negligible for $0.23 < z < 0.38$. Morphologically, the LRG are bulge-dominated galaxies, and have surface brightness distributions and stellar light concentrations similar to those present day giant ellipticals and lenticulars. The LRG spectra match the spectral energy distribution of an old stellar population, although there are unresolved issues regarding non-solar abundance ratios (Eisenstein et al. 2003).

However, the LRG target selection algorithm only yields a consistent population of galaxies for $z > 0.23$. At lower redshift, the color criteria do not distinguish between less luminous and intrinsically bluer galaxies from the desired luminous and red ellipticals. However, luminous red ellipticals with $z < 0.23$ are bright enough to be included in the main SDSS galaxy sample (Strauss et al. 2002) of which rest frame colors and luminosity to select a consistent population. We use an empirically determined color-redshift relation, described in Appendix A And outlined in full in Loh et al. (2005a), to select $z < 0.23$ galaxies with the same evolution-compensated rest-frame color and luminosities as the higher-redshift LRGs.

Figure 1 shows the histogram of the comoving density of LRG before and after we do the consistent rest-frame selection. Our sample has essentially a constant density, and is thus volume-limited from $z \approx 0.12$ up to roughly $z \approx 0.38$. The low redshift limit is a consequence of the bright-end incompleteness of the SDSS spectroscopic survey, as the SDSS spectrographs show excessive crosstalk when the flux within the $3''$ fiber exceeds $r \sim 15$ (or $r_{\mathrm{petro}} \sim 13.5$). The high redshift limit comes from the LRG faint

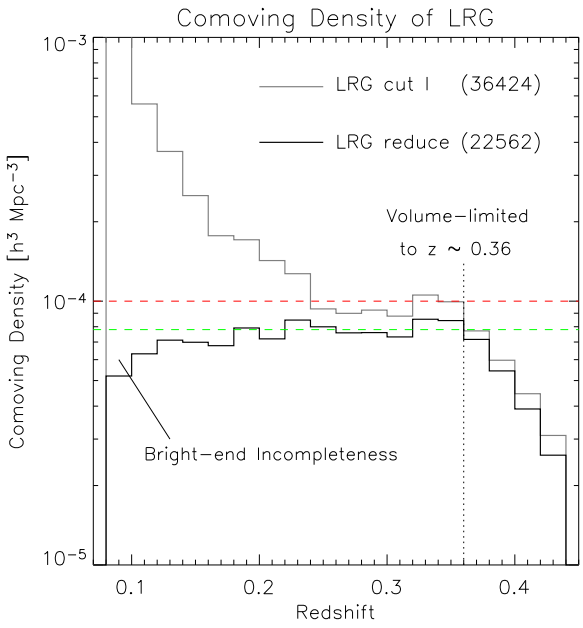

Figure 1. The comoving density of LRG (Cut I) as a function of redshift before (grey) and after (black) applying the consistent rest-frame color and luminosity cut as described in Appendix A. The new trimmed LRG sample is approximately volume-limited to $z \approx 0.38$ with a density of $\sim 8 \times 10^{-5} h^3\,\mathrm{Mpc}^{-3}$.

magnitude limit of $r_{\rm lim} = 19.2$. The comoving density of these galaxies is $\sim 8 \times 10^{-5} h^3\,\mathrm{Mpc}^{-3}$, an order of magnitude larger than the abundance of Abell (1965) Richness Class $\geqslant 0$ clusters of galaxies, and roughly matches the expected abundance of haloes with mass greater than $5 \times 10^{13}\,h^{-1}\,M_\odot$ given a concordance power spectrum.

Our primary spectroscopic data are derived from the uniform large-scale structure compilation `sample12` of Blanton et al. (2004); this covers $2099\,\mathrm{deg}^2$ of sky. A thorough discussion of this sample is given in the appendix of Tegmark et al. (2004) and Blanton et al. (2004). There are $12,608$ LRG with $0.12 < z < 0.38$ in `sample12` that pass the consistent population rest-frame magnitude and color cuts described in Appendix A. We refer to this as the *trimmed* LRG sample. To determine the environments of the LRG in this sample, and to measure the dominance of the BCG, we use imaging data from the SDSS DR1. We consider all sources that are classified as galaxies by the SDSS photometric pipeline `photo` with $r_{\rm petro} < 21.0$, a level at which the photometry is of very high S/N, and at which star-galaxy separation is particularly clean (Scranton et al. 2002). $r_{\rm petro}$, the Petrosian (1976) magnitude in the SDSS r-bandpass, is the primary extended source flux measurement used in this paper; see Strauss et al. (2002) for a complete discussion. All magnitudes and colors are corrected for Galactic extinction using the Schlegel, Finkbeiner & Davis (1998) map and assuming $R_V = 3.1$.

3 STATISTICAL TESTS OF THE LUMINOSITY FUNCTION TAIL

The observed narrow luminosity and color distribution of BCGs (Postman & Lauer 1995), and the possible influence of dynamical friction and tidal stripping in their evolution, suggest that their luminosity function may be distinct from that of the field. This is often framed in terms of *statistical* versus *special* luminosity functions: the former argues that BCGs are a mere statistical extreme of the luminosity function of cluster ellipticals, while in the latter, the BCG forms a different class, having its own unique distribution shared among BCGs in many clusters.

Tremaine & Richstone (1977) have developed an elegant test to distinguish between these two descriptions; this method does not require the determination of the galaxy luminosity functions of the individual clusters involved. Readers who are interested in the detailed derivation of the theorems that support the validity of the test should refer to their paper. The test hinges on two key assumptions about the nature of the galaxy luminosity distribution in clusters. The first is Scott (1957)'s model for the luminosity function, which postulates that for a given luminosity distribution, overlapping magnitude intervals are statistically independent. If ψ is the integrated luminosity function

$$\psi(m) \;=\; \int_{-\infty}^{m} \phi(m')\,\mathrm{d}m'\,, \tag{1}$$

then the probability of finding ν galaxies in the magnitude interval $[m_a, m_b]$ is

$$p_\nu(m_a, m_b) \;=\; \frac{\left[\psi(m_b) - \psi(m_a)\right]^\nu}{\nu\,!} \exp\left[\psi(m_a) - \psi(m_b)\right] \tag{2}$$

The number, ν, of galaxies (within a single isolated cluster) is a *Poisson* variate with mean and variance $\psi(m_b) - \psi(m_a)$. In the case of finding a single galaxy in the infinitesimal interval $[m, m + \mathrm{d}m]$, equation (2) reduces to

$$\mathrm{d}P \;=\; p_1(m, m+\mathrm{d}m) \;=\; \phi(m)\,\mathrm{d}m \tag{3}$$

In this model, the probability distribution of the j-th ranked galaxy with magnitude m, $p_{(j)}(m)\mathrm{d}m$, is just[2]

$$\begin{aligned} p_{(j)}(m)\,\mathrm{d}m \;&=\; \mathrm{prob}\left\{j-1 \text{ galaxies brighter than } m\right\} \\ &\quad \times \mathrm{prob}\left\{\text{one galaxy in } (m, m+\mathrm{d}m)\right\} \\ &=\; p_{j-1}(-\infty, m) \times p_1(m, m+\mathrm{d}m) \\ &=\; \frac{\psi(m)^{j-1}}{(j-1)\,!} \exp[-\psi(m)]\,\phi(m)\,\mathrm{d}m \end{aligned} \tag{4}$$

Scott's model thus states that galaxy luminosities are drawn from a Poisson distribution, with magnitudes m being treated as independent random variables. This is completely embodied in equation (4).

The second assumption is that the bright end of the luminosity function drops off as a power-law (exponentially in magnitude), which allows one to write down an explicit analytical expression for the luminosity distribution of the nth-ranked galaxy. For example, the probability distribution of the luminosity of the first-ranked galaxy with a universal bright end differential luminosity function $\phi(m) \simeq \exp[\alpha(m - m_0)]$ is

$$\begin{aligned} p_{(1)}(m)\,\mathrm{d}m \;&=\; \exp[-\psi(m)]\,\phi(m)\,\mathrm{d}m \\ &\simeq\; \alpha \exp[\alpha(m-m_0) - e^{\alpha(m-m_0)}]\,\mathrm{d}m. \end{aligned} \tag{5}$$

Here, α parameterizes the steepness of the function, and m_0 gives the normalization (or richness) of the cluster.

Early studies by Peebles (1968); Peterson (1970); Geller & Peebles (1976); Schechter & Peebles (1976) that

[2] Numbers in parentheses, e.g. $m_{(j)}$, indicate (j-th) ranked variables.

compared observed ranked magnitude distributions with Scott's model prediction (equation (5) and its extension to higher ranks) were inconclusive. This is because the catalogs used in these studies had insufficient redshift information and reliable cluster membership for even the brightest few galaxies. In addition, small uncertainties in the relative *k*-correction in clusters at various distances wash away subtle effects that would otherwise distinguish the statistical and special descriptions of the BCG luminosity distribution.

3.1 The Magnitude Difference Between First and Second-Ranked Galaxies

Tremaine & Richstone's key insight was to realize the importance of using the magnitude differences for a statistical test. The exponential cutoff in the differential luminosity function $\phi \sim \exp(\alpha m)$ not only predicts the expected distribution of the first-ranked magnitudes (equation 5), but also puts a tight constraint on the expected distribution of the *differences* between the ranked magnitudes. BCGs (the first-ranked members) are observed to have a small spread in magnitude, $\sigma(M_1) < 0.3$ (Sandage 1972; Postman & Lauer 1995), suggesting that on average, the magnitude difference between the first-ranked galaxy, and their respective second-ranked galaxies, $M_{12} \equiv M_2 - M_1$, cannot be too large, if both of these galaxies are drawn from the same exponentially decaying ϕ. Indeed, Tremaine & Richstone showed that the expected magnitude difference, $\langle M_{12} \rangle$ must at most be of the same order as the size of the spread of the first ranked galaxy magnitudes:

$$T_1 \equiv \frac{\sigma(M_1)}{\langle M_{12} \rangle} \geqslant 1 \, . \tag{6}$$

Similarly, they showed that the spread of the magnitude difference, $\sigma(M_{12})$, must also be of the same order of magnitude as the difference $\langle M_{12} \rangle$:

$$T_2 \equiv \frac{\sigma(M_{12})}{\langle M_{12} \rangle} \gtrsim 0.82 \, . \tag{7}$$

The two inequalities are valid even when there are variations in the bright end slope α_i of each of the clusters of galaxies used to derive the distributions of M_1, M_2, M_{12} etc., so long as the ϕ_i satisfy the two assumptions discussed above. Note that equation (5) holds only under the more restrictive assumptions that all α take a single value, and that the intrinsic richness of the clusters, m_0 be the same.

However, in the limit that all the $\alpha_i \to \langle \alpha \rangle < 0$, the magnitudes, m, of Scott's model would be an identical and independently distributed (i.i.d) random variable. Using extreme-value statistics, Bhavsar & Barrow (1985) showed that as long as ϕ has a general functional form in the *domain of attraction* of the exponential distribution – including the Gaussian, Gamma, exponential and double-exponential distributions, then equation (5) is the expected distribution for statistical BCG, and the expectation value for our two statistics are $\langle T_1 \rangle \simeq 1.28$ and $\langle T_2 \rangle \simeq 1.0$. It is remarkable that both these values are independent of both α and m_0.

Note that the statistic T_2 depends solely on the differential quantity M_{12}, and eliminates uncertainties associated with redshift and direction dependent corrections like *k+e* and extinction, making analyses that combine data from different epochs more robust.

4 MEASUREMENT OF M_1, M_2 AND RICHNESS OF LRG ENVIRONMENTS

The trimmed LRG spectroscopic sample we are using extends to $z = 0.38$. However, the main SDSS galaxy sample, probing lower-redshift galaxies, has a median redshift of only ~ 0.1, with very few galaxies above $z = 0.2$. We therefore use the *photometric* data from the SDSS to characterize the environments and the luminosity distribution of galaxies around each LRG, and to calculate statistics such as M_{12}. We do so by using color cuts to isolate early-type galaxies at the same redshift as the LRG, using the red sequence seen in cluster color-magnitude diagrams. Within an angular extent equivalent to $1.0\,h^{-1}\,\mathrm{Mpc}$ at the redshift of each spectroscopic LRG, we searched the SDSS photometric data for second- and third-ranked galaxies with $g-r$ and $r-i$ colors typical of early-type galaxies at that redshift. The regularity of the observed color-magnitude relation of early-type galaxies seen out to $z \sim 0.5$ and beyond, e.g. Blakeslee et al. (2003), enables us to empirically determine a color-redshift locus for these galaxies. This is shown in Figure B1, with an estimated dispersion at each redshift given by the solid ellipses. Details of how this locus is determined is described in Appendix B. Note that the locus is not simply drawn from the colors of LRG themselves since "Cut I" LRGs are red biased – lower luminosity galaxies need to have a redder color to pass the selection cut (Eisenstein et al. 2001). The ellipses include the observed color errors – almost entirely due to photometric scatter[3] – of galaxies on the red sequence with apparent magnitude brighter than $\sim M^*(z)$ at each redshift. Hence, if we include only galaxies from the fields around each LRG with colors within the $n^{\mathrm{th}}\,\sigma$ ellipse of the LRG redshift, then on average, we will be complete with respect to red sequence galaxies in the LRG fields at the $n\,\sigma$ level. Of course, for larger n, the background contamination goes up. We find that the contamination remains manageable, while still including the majority of galaxies in the red sequence, if we include galaxies that are within $2.5\,\sigma$ of the color locus.

The galaxies are then ranked by apparent Petrosian r magnitude. The first-ranked galaxy in each field is the LRG 95–99% of the time, with the lower values holding in higher redshift fields. In some of the exceptions, the first-ranked galaxy was also flagged as an LRG candidate, but a spectrum was not obtained because of the restriction that two spectroscopic fibers not be placed closer than $55''$ (Blanton et al. 2003a). The majority of the remainder turned out to be bluer galaxies presumably in the foreground, selected because of the generosity of the $2.5\,\sigma$ color cut. We keep this small number of non-LRG first-ranked galaxies in our analysis so as not to bias our result against the occasional true bluer first-ranked galaxy. However, excluding them from our sample does not significantly change our results.

Our first goal is to derive the intrinsic joint distribution of M_1 and M_{12}, $\phi(M_1, M_{12})$. For this, we need to estimate and subtract the background distribution $\phi^{\mathrm{back}}(M_1, M_{12})$. For each LRG field, we select ten random positions within the same SDSS imaging `stripe` (York et al. 2000). Just as in the LRG fields, we draw a $1.0\,h^{-1}\,\mathrm{Mpc}$ circle, apply the same $2.5\,\sigma$ red sequence color cut, and rank the galaxies by brightness. The ϕ are binned with $\Delta M_1 = 0.1$ `mag` and $\Delta M_{12} = 0.2$ `mag`. Figures 2 and 3 show the composite ϕ for 271 and 1732 LRG fields at $0.14 < z < 0.16$, and $0.34 < z < 0.36$, respectively. The top left panel of each

[3] The intrinsic scatter of the color-magnitude relation is expected to be less than 0.05 magnitude even at $z = 0.4$ (Ellis et al. 1997; Cool et al. 2005; Loh et al. 2005a).

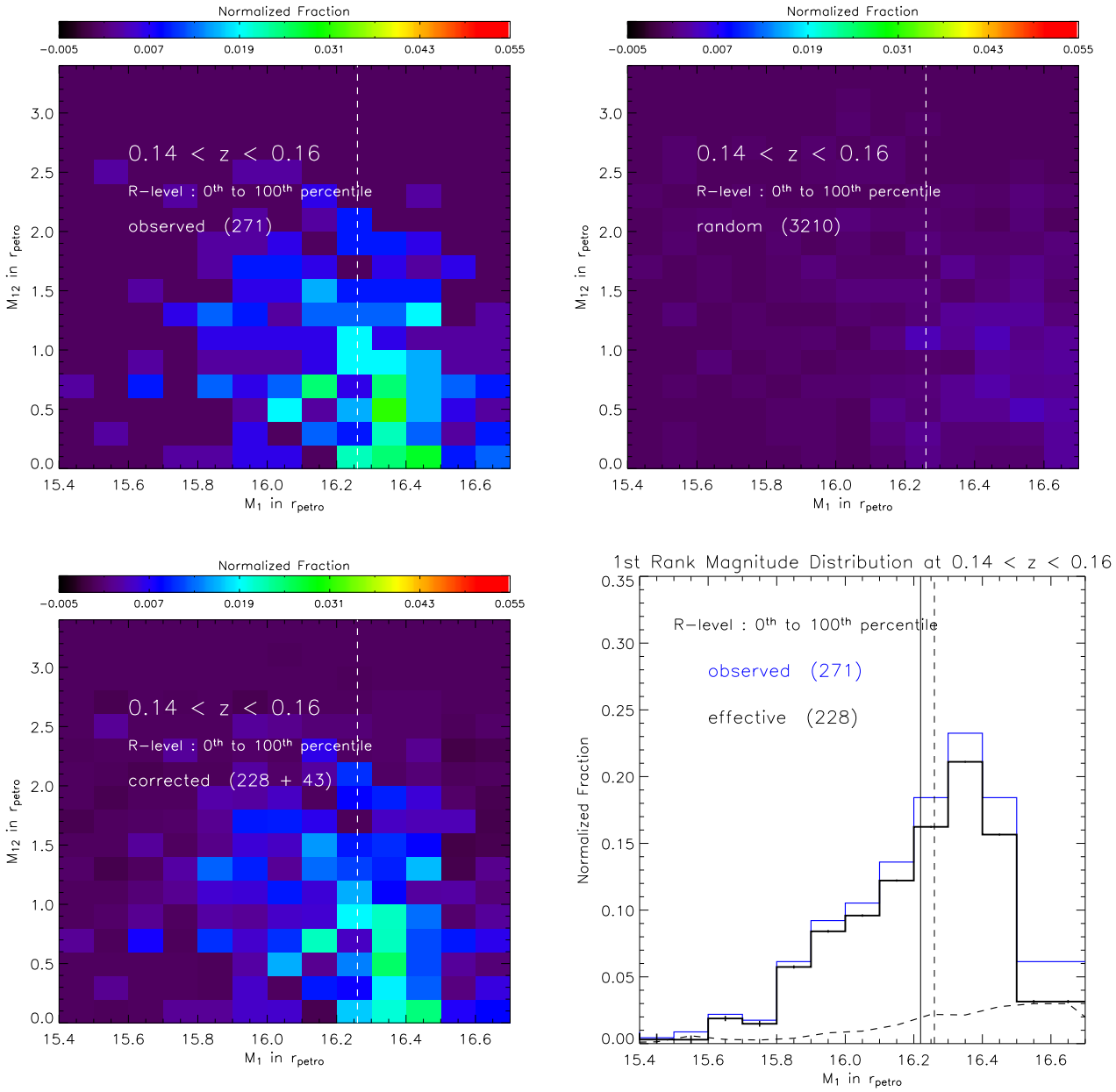

Figure 2. These figures illustrate the background subtraction in M_1 and M_{12} space, done in a narrow redshift interval of $0.14 < z < 0.16$. The top left panel gives the observed composite $\phi(M_1, M_{12})$ for 271 LRG fields; top right is the background estimated from 3210 random positions, but scaled by area to match the observed $\phi(M_1, M_{12})$. The bottom left panel is the corrected distribution using equation (8), weighting by $f = 228/271$, the ratio of the number of uncontaminated (effective) fields to the total observed fields. The bottom right gives the marginalized 1st ranked distribution. The blue histogram is the observed $\phi(M_1)$ distribution, and the black histogram is the effective distribution obtained by subtracting the (dashed) background. The solid vertical line gives the mean $\langle M_1 \rangle$. The magnitude of a $M^* - 1.5$ early-type galaxy at the median redshift of $z \sim 0.15$ is indicated by the dashed vertical line in all panels. Density contours and histograms are normalized to unity.

figure is the observed distribution while the bottom left gives the background. The dashed vertical line is the observed magnitude of a $M^* - 1.5$ galaxy at the respective redshift, while the slanted solid line gives the upper bound to the M_{12} we could observe given the SDSS photometric catalog limit of $r_{\rm petro} = 21.0$. Between 0.5% and 1% of all LRG in our sample are isolated (see Loh et al. 2005b for further discussion), showing no companion within the color and magnitude space we searched. These objects may well be fossil groups (Ponman et al. 1994), showing substantial numbers of low-luminosity companions below our photometric limits. We leave the study of these objects to a future paper.

We estimate the intrinsic distribution in M_1 and M_{12} (given in the top right panels) using a weighted subtraction given by

$$\hat{\phi}\,(M_1, M_{12}) \;=\; f \times [\phi^{\rm obs}(M_1, M_{12}) - \phi^{\rm back}(M_1, M_{12})] + (1-f) \times \phi^{\rm obs}(M_1, M_{13}) \qquad (8)$$

where $f \equiv (N_{\rm obs} - N_{\rm back})/N_{\rm obs}$ is the fraction of fields in which M_{12} measurements are not affected by contamination, and $N_{\rm obs}$

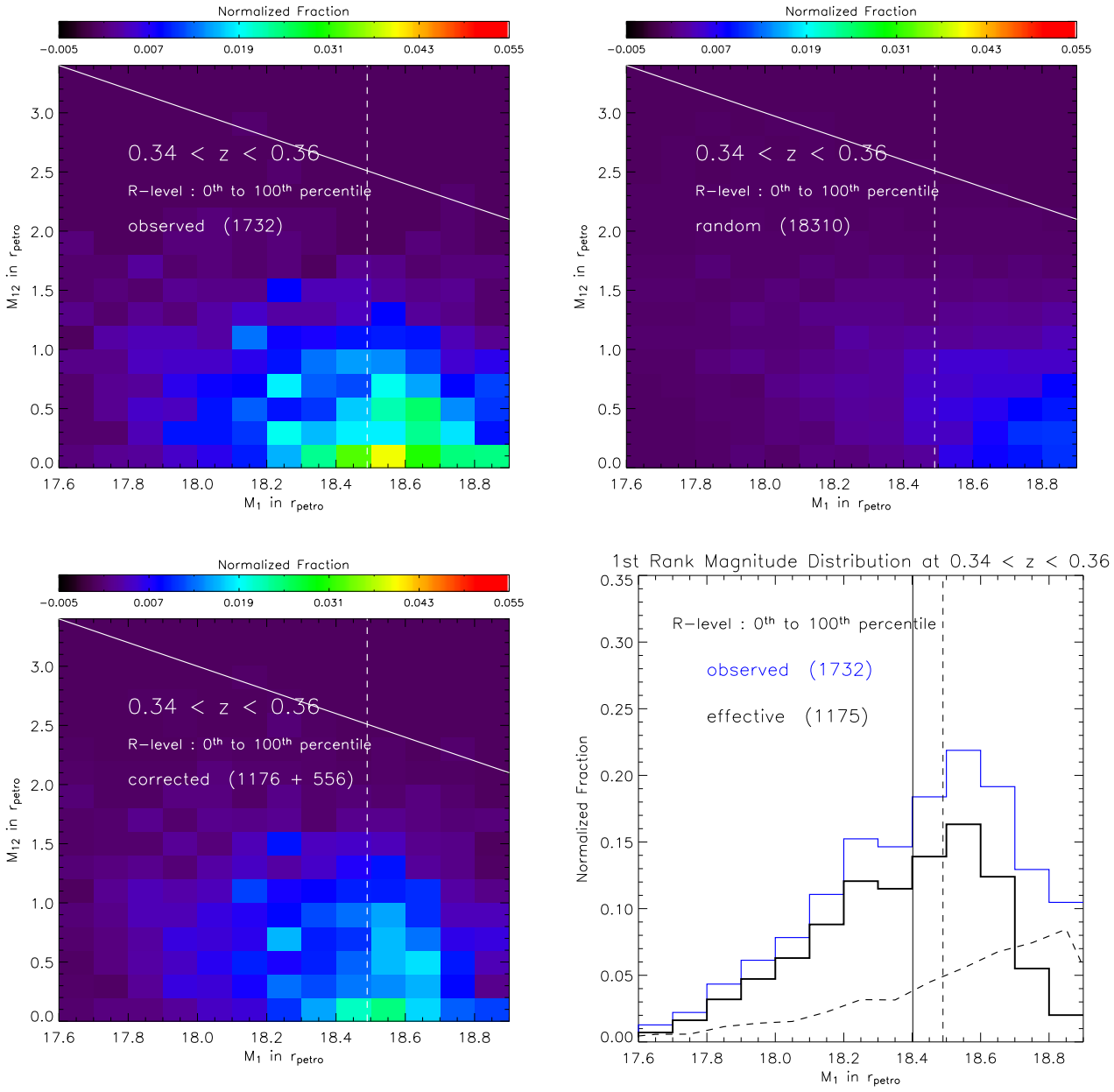

Figure 3. As in Fig. 2; for $0.34 < z < 0.36$. The solid diagonal line in the 2D plots gives the upper bound of M_{12} for a given M_1 set by the flux limit ($r_{\rm petro} < 21.0$) of the SDSS imaging catalog.

and $N_{\rm back}$ are the number of LRG and background fields in the M_1, M_{12} bin in question. If the background contamination $(1 - f)$ is large, there is a substantial probability that the galaxy we've labelled the second-ranked is actually a background (or foreground) object, thus what we have labelled the third-ranked galaxy is in fact M_2. This is the origin of the second term in equation (8).

We first perform our analysis on the full volume-limited trimmed sample of LRG in a series of redshift intervals of width $\Delta z = 0.02$ from $z = 0.12$ to $z = 0.38$. We define the richness (or the associated galaxy overdensity) of each LRG field by counting the number of galaxies on the red sequence within $1.0\,h^{-1}\,{\rm Mpc}$ of the LRG from $M^* - 2.5$ down to M^* (Loh et al. 2005b). We then split the sample into four, in terms of quartiles based on the richness of these LRG fields; the richness ranking is done within each redshift slice. We term the relative rank of each LRG in its redshift slice the R-level. The upper quartile sample, with a median of 8 early-type galaxies with magnitude M^* and brighter within a $1.0\,h^{-1}\,{\rm Mpc}$ radius, are the equivalent of a present day moderately rich cluster of galaxies (e.g. Abell (1965) Richness Class > 1). Objects in the $25^{th} - 50^{th}$ percentile, on the other hand, with 2 to 3 galaxies on the red sequence, are similar to present day groups of galaxies.

Figure 4 is the redshift histogram of LRG used for our analysis. The blue shading refers to the upper quartile, while the red shading indicates the $25^{th} - 50^{th}$ percentile. Note that the fraction of LRG fields in the upper quartile (say) of a given redshift subsample can be greater or smaller than 25% of the subsample total because LRGs with the same richness share the same rank.

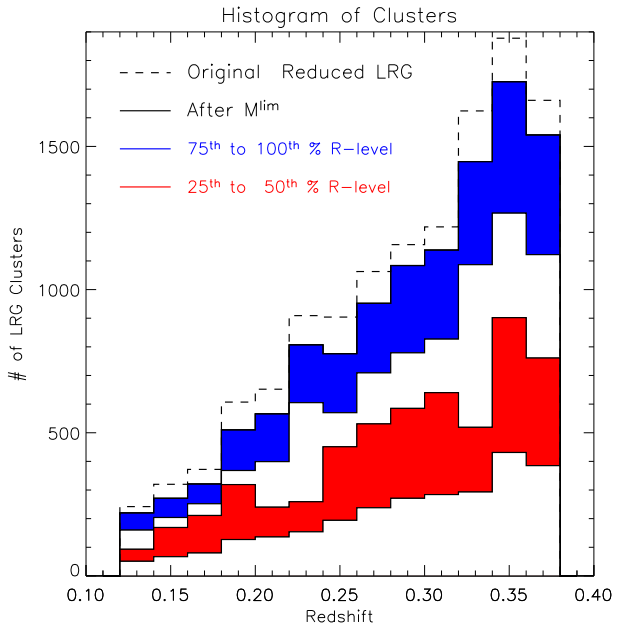

Figure 4. Redshift histogram of the trimmed LRG sample. The blue (red) shading indicate the number of LRG fields with richness in the upper $75^{\rm th}(25^{\rm th}-50^{\rm th})$ percentile.

5 TREMAINE-RICHSTONE STATISTICS AS FUNCTIONS OF REDSHIFT AND RICHNESS

Figures 2 and 3 show that as one goes to higher redshift, LRG clusters tend to have smaller M_{12}. For example, at $z \approx 0.15$, there are quite a few LRG clusters with $M_{12} \sim 2$, well above the noise level (given by the bottom left panels), while there are no clusters with such a large gap at $z \approx 0.35$.

This systematic smaller gap at higher redshift is also seen when the sample is split into group-like ($25^{th}-50^{th}$) and cluster-like (upper quartile) LRG fields, as shown in the top panels of Figures 5 and 6. The bottom panels of each figure show histograms of the marginal gap distribution, $\phi(M_{12})$, explicitly showing the noise level, $\phi^{\rm back}(M_{12})$ (dashed) determined from 10 random positions for each LRG, the observed $\phi^{\rm obs}(M_{12})$ (blue) and $\phi^{\rm obs}(M_{13})$ (red), and the final distribution $\hat{\phi}(M_{12})$ (solid) used for our analyses as estimated from equation (8). The vertical dashed line is the mean $\langle M_{12}\rangle$ for each panel, estimated from the first moment of $\hat{\phi}(M_{12})$. It shows a slight decrease with redshift for both clusters and groups.

The Bautz & Morgan (1970) effect, whereby clusters with brighter BCGs have larger gaps, is seen in both rich and poor systems at all redshifts. One measure of the strength of this effect is the tilt of the number density ellipsoid of the joint distribution, $\phi(M_1, M_{12})$. From Figures 5 and 6, it appears that this effect is stronger in poorer systems, but changes little with redshift.

LRG fields with group-like environments have a larger gap than do cluster-like environments at all redshifts. This is seen in both the joint distribution, $\phi(M_1, M_{12})$, and marginal distribution, $\phi(M_{12})$ (Figures 5 and 6). This must in part be statistical: Poisson sampling from a common luminosity function naturally gives a smaller gap for a larger total number of galaxies. We will see below from the Tremaine-Richstone statistics that this is not the whole story; Figure 8 shows that the bounds of equations (6) and (7) are violated. If the universal galaxy luminosity function estimated over large scale (cf. Blanton et al. 2003a) is correct, i.e. the bright end cuts off exponentially like a Schechter function, then the Poisson assumption must not hold.

Figure 7 summarizes the evolution of the mean and dispersion of M_1 and M_{12} from the various sub-samples. The top right panel shows that poorer systems have first-rank members that are brighter by 0.1–0.2 mag in the mean, while the top left panel shows that these same systems have a larger mean $\langle M_{12}\rangle$ at all redshifts. Our sample is volume-limited independent of richness, and the second and third ranked galaxies are also complete for the range of M_{12} and M_{13} we are probing, given the depth of the SDSS photometric data. The dependence of the gap size on richness is not an artifact of our richness estimates, as the mean (and median) number of M^* and brighter galaxies is roughly constant with redshift, after background subtraction (cf. Loh et al. 2005b).

Our results for the Tremaine & Richstone statistics T_1 and T_2 are presented in Figure 8. The estimated $\hat{T}_1$ and $\hat{T}_2$ are well below the lower bounds for the statistical BCG hypothesis (indicated by the solid horizontal line) set by equation (6) and (7) for both poor and rich systems at all redshifts. They are even further away from the statistical i.i.d. prediction (upper dashed line) from extreme-value statistics of Bhavsar & Barrow (1985). If we assume that the bright end of the galaxy luminosity function in clusters cuts off exponentially like the universal galaxy luminosity function, then the statistical hypothesis for BCG is rejected with high confidence, even if we allow the steepness of this cut-off to vary from cluster to cluster. Of course, this result has meaning only if our initial assumption about the galaxy luminosity function embodied in Scott's model – of independent luminosity sampling – is valid. The assumption that the luminosities of galaxies are independent must break down at some level, since we know that galaxies influence with each other via tidal interactions and mergers through gravity to very large distances. On the scale of $1.0\,h^{-1}\,{\rm Mpc}$, the independence assumption is unlikely to be true especially for galaxies as massive as LRGs ($\sim 5-8\times10^{12}M_\odot$). Hence the fact that T_1 and T_2 fall well below the boundaries of equations (6) and (7) does not by itself imply that BCGs follow an assembly path different from that of other cluster galaxies. It might merely signal a breakdown in our assumption about the galaxy luminosity function. Indeed, bright elliptical galaxies, including BCGs (Oegerle & Hoessel 1991; Postman & Lauer 1995; Graham et al. 1998) form a low dimensional sequence (the Fundamental Plane relation, Dressler et al. 1987; Djorgovski & Davis 1987), implying some kind of universal assembly history.

T_1 and T_2 are the inverse of the mean luminosity ratio of the two brightest galaxies, measured in units of the two characteristic luminosity spreads, $\sigma(M_1)$ and $\sigma(M_{12})$. When considered as a function of redshift, they quantify the *normalized* relative brightening of the first-ranked galaxy, as compared with lesser members of the same cluster. These normalizations are with respect to the dispersions of M_1 and M_{12}. $\hat{T}_1(z)$ and $\hat{T}_2(z)$ are consistent with being flat as a function of redshift, suggesting that there is no major process that influences the creation of the observed luminosity gap over the redshift range we probe. This can be compared with the raw gap function, $\langle M_{12}\rangle(z)$, of the top left panel in Figure 7, where a decrease with redshift is seen, suggesting mild brightening of the first-ranked galaxy compared to the second-ranked galaxy with time. Nonetheless, the corresponding spread in magnitude, notably $\sigma(M_{12})$, also decreases with redshift, in such a way that $\hat{T}_2$ remains flat.

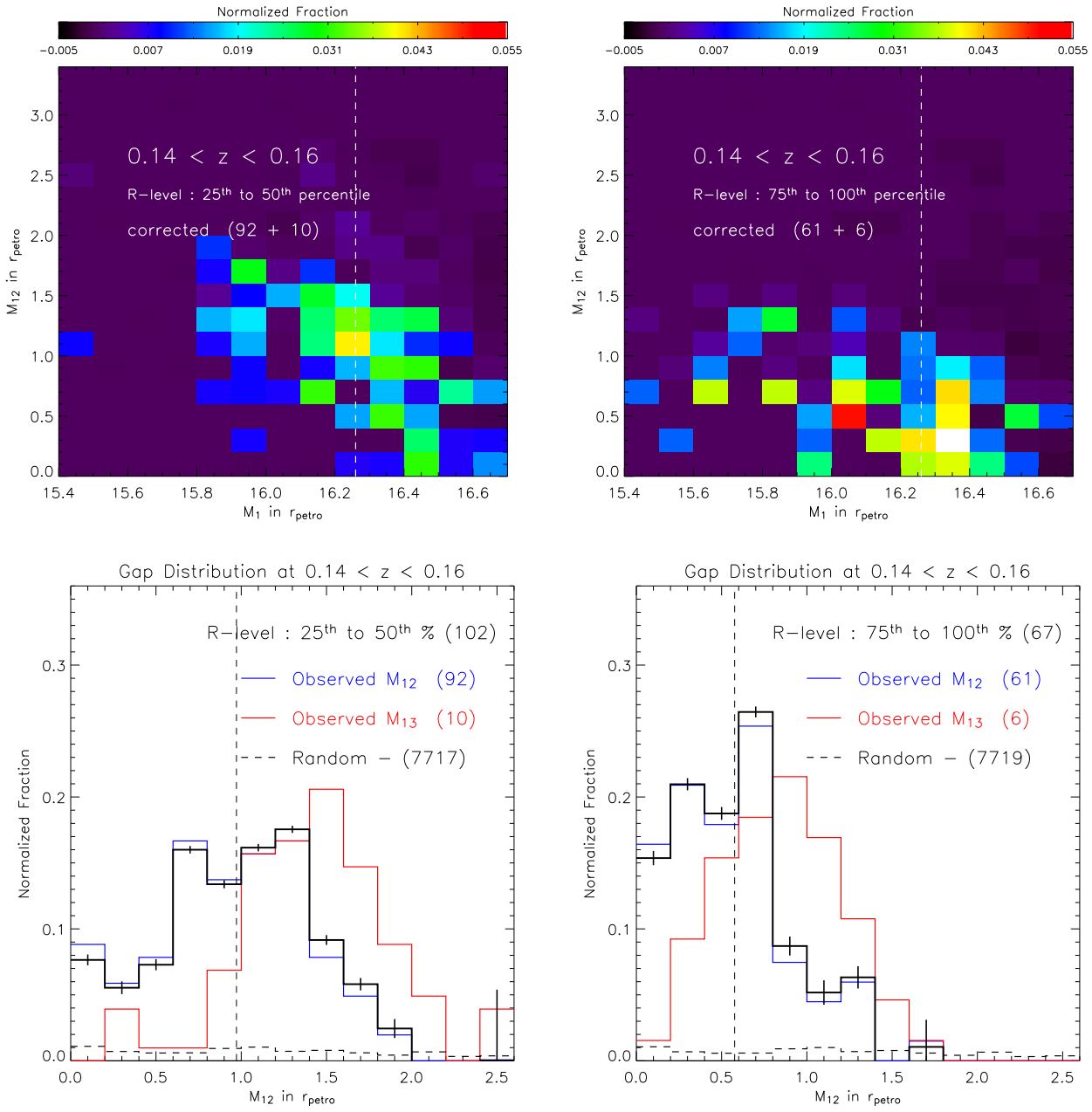

Figure 5. On the top left (right) panel is $\phi(M_1, M_{12})$ for LRG fields with richness R-level in the $25^{\rm th}$ to $50^{\rm th}$ ($75^{\rm th}$ and above) percentile. Higher percentile corresponds to richer systems. The bottom panels are the corresponding marginalized $\phi(M_{12})$. The black histogram is the final distribution estimated from equation (8) – a weighted linear combination of the observed M_{12} (blue) and (M_{13}) (red) distribution, and the background distribution (dashed). For LRG fields with redshifts $0.14 < z < 0.16$.

6 DISCUSSION

6.1 Interpretive Caveats

Our richness measure says little about the gravitational potential of the LRG fields, since we do not measure the mass overdensity directly. Our proxy for overdensity, the R-level yardstick, is tuned to robustly characterize the environment of rich systems with high signal-to-noise ratio. Our groups (i.e., the $25^{\rm th} - 50^{\rm th}$ percentile sample) by design must host a luminous ($\lesssim M^* - 1$ or brighter) LRG, hence it is a highly biased sub-class of galaxy groups. The comoving number density of our groups is a mere $2 \times 10^{-5} h^3\,{\rm Mpc}^{-3}$, an order of magnitude below the expected group density from the analytical Press & Schechter (1974) estimates. Hence, we do not sample a substantial fraction of group-like environments in the universe. Even if the mass–to–R-level scaling relation is tight and unbiased (Loh et al. 2005c), our richness measurements can give biased mean mass estimates in the present of moderate intrinsic scatter and measurement uncertainties. Further, it could be that our groups are equally massive, with a huge dwarf galaxy population compared to their richer counterparts, as observed locally in a subset of X-ray bright Hickson compact groups (Hunsberger, Charlton & Zaritsky 1998).

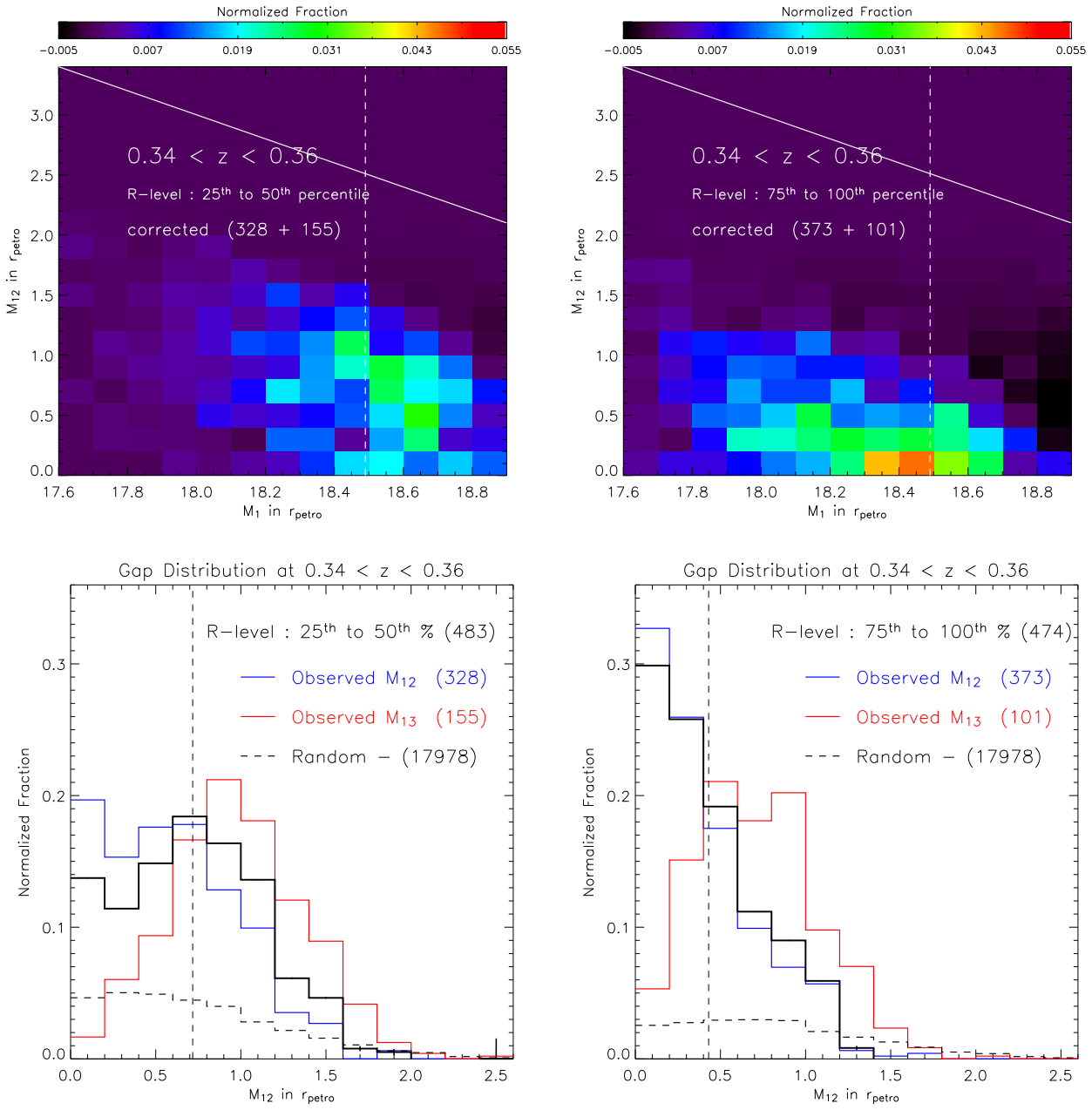

Figure 6. As in Fig. 5, for redshifts $0.34 < z < 0.36$.

These groups are higher redshift analogs of the famous Morgan, Kayser & White (1975) and Albert, White & Morgan (1977) groups that host luminous (non-c) D galaxies. However, we are only sampling a subset of special groups, which may resolve the apparent contradiction between our results and those of Geller & Postman (1983) – they found that the brightest members of groups are less dominant than those of clusters and are consistent with them simply representing the luminous tail of the luminosity function. It would be of interest to know what fraction of *all* groups (observationally defined) host an LRG. We will show in a subsequent paper (Loh et al. 2005c) that $\sim 95\%$ of the most massive clusters selected by both the optical matched-filter techniques (Kim et al. 2002a) and X-rays have LRGs in them, but the fraction for groups is expected to drop substantially. Note that the number density of groups from optical redshift surveys have a higher number density than LRGs, in part because many of these groups are not actually virialized and display no extended X-ray emission. Further, there are groups with extended X-ray emission that have bright elliptical members that are just shy of the $M^* - 1$ luminosity threshold of the LRG (Nipoti et al. 2003).

Another caveat of our analysis is the $1.0\,h^{-1}\,\mathrm{Mpc}$ scale used to search for second and third ranked galaxies. If we choose a smaller scale, say $0.25h^{-1}\,\mathrm{Mpc}$, we find a larger mean gap for both richer and poorer system, by ~ 0.5 `mag`. However, the difference in the gap between rich and poor systems is smaller. For example, at the current $1.0h^{-1}\,\mathrm{Mpc}$ scale, the average difference of the estimated $\langle M_{12} \rangle$ between the rich and poor systems is 0.4 `mag` (see the top right panel of Figure 7), while at $0.25h^{-1}\,\mathrm{Mpc}$

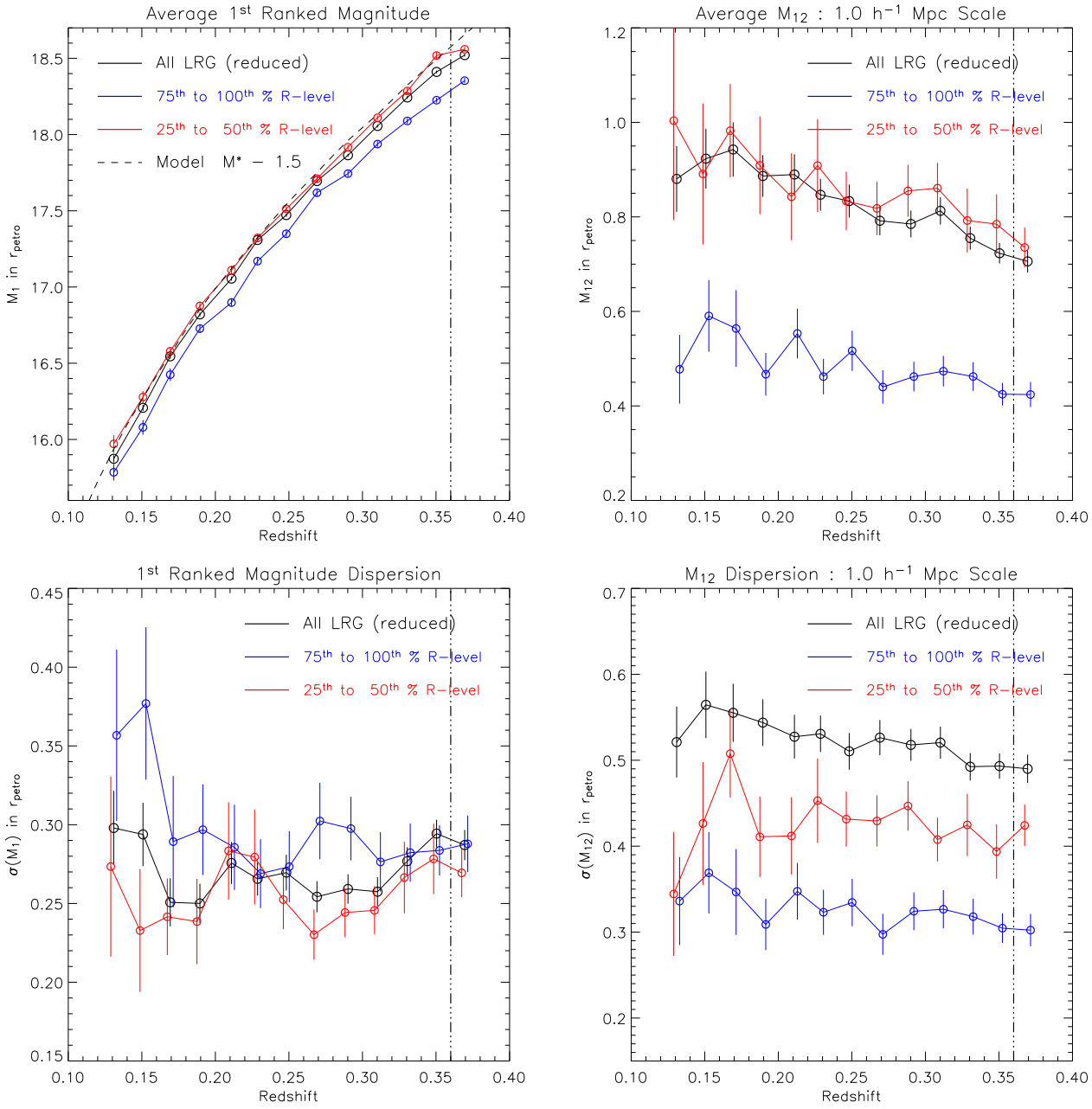

Figure 7. (Left Panels) Average $1^{\rm st}$ ranked $r_{\rm petro}$ magnitude (top) and its corresponding $1\,\sigma$ dispersion (bottom) as a function of redshift. (Right Panels) $\langle M_{12}\rangle$ and its corresponding $1\,\sigma$ dispersion as a function of redshift. The blue (red) is for fields with richness in the upper $75^{\rm th}(25^{\rm th}-50^{\rm th})$ percentile. Errors bars are 1σ from bootstrap. The dot-dashed line is at $z=0.36$, the redshift beyond which the sample is no longer volume-limited.

it is ~ 0.15 mag. This difference is again in part Poissonian, but is also influenced by how bright galaxies populate a cluster. The smaller scale analysis of $0.25h^{-1}\,{\rm Mpc}$ would, for example, split the Coma cluster into two LRG fields, each with a large luminosity gap, while the present $1.0h^{-1}\,{\rm Mpc}$ analysis would treat Coma as a single system with a small gap. We could try to infer a dynamically motivated scale like a virial radius or r_{200} – the radius at which the galaxy density drops below 200 times the mean density – but these measurements are noisy and ill defined for poor systems.

6.2 Comparison with Numerical Studies

We compare our findings with the numerical experiment of Dubinsky (1998), who simulated the formation of groups and poor clusters of galaxies in a cosmological setting (albeit based on the now out-of-favor $\Omega_m = 1, \sigma_8 = 0.7$ CDM model). Our $25^{\rm th}-50^{\rm th}$ percentile R-level sample matches his systems. His simulation specifically addresses the growth of the brightest galaxy and its creation in the context of cluster collapse in a hierarchical structure formation paradigm. His experiment begins at $z=2$, and by $z\sim 0.8$ the major galactic unit that is later identified as the BCG is already in place. This BCG is a result of mergers of the brightest few galaxies of roughly equal mass during the triaxial

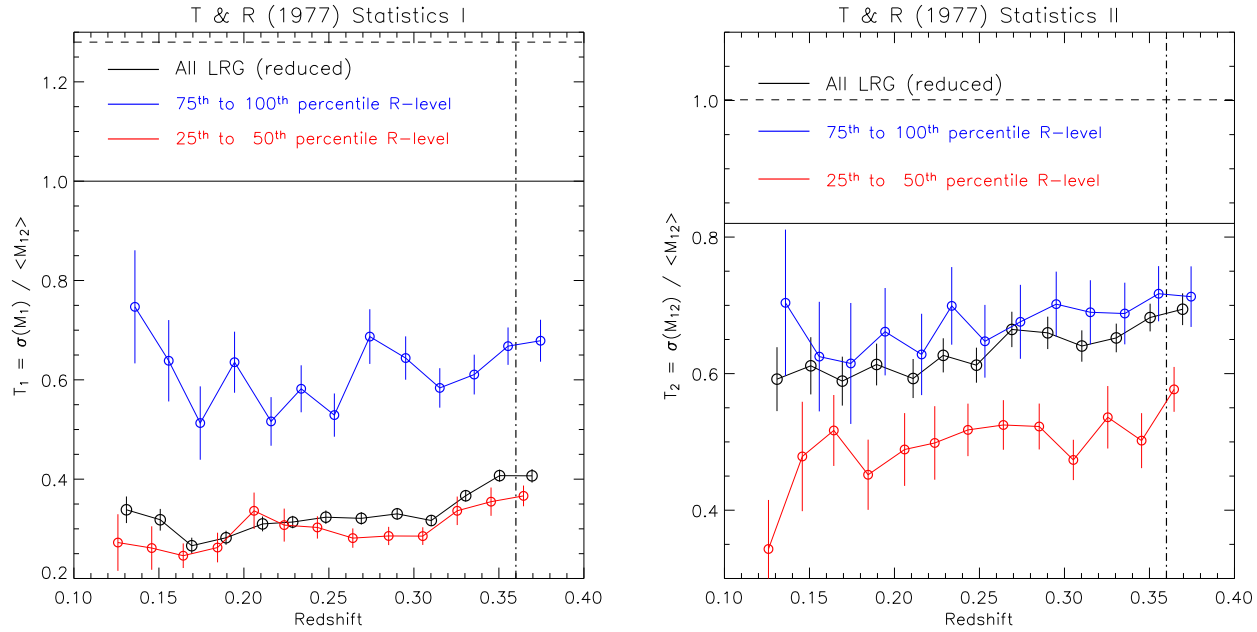

Figure 8. The Tremaine & Richstone (1977) statistics T_1 and T_2 as a function of redshift computed in redshift slices $\Delta z = 0.02$. The solid horizontal line gives bounds below which brightest members would cease to be the statistical extreme of the luminosity function of lesser members in the cluster. The top dashed line is the prediction from extreme-value statistics. The blue (red) curve is for fields with richness in the upper $75^{\rm th}(25^{\rm th} - 50^{\rm th})$ percentile. Errors bars are 1σ from bootstrap. The dot-dashed line is at $z = 0.36$, the redshift beyond which the sample is no longer volume-limited.

collapse of the cluster. By $z \sim 0.4$, all major mergers between the BCG and other galactic units are complete. The large mass contrast between the BCG and the second-ranked galaxy is now in place. This would suggest that M_{12} will shrink at $z > 0.4$, unfortunately beyond the redshift which our sample probes. Qualitatively, our results from the group-like LRG fields are in agreement with his numerical experiment. The large and unchanging gap seen in these poorer systems points to an earlier origin of the growth of the dominance of the BCG, of which the picture painted by his experiment is one plausible description. However, cluster infall and growth is a strong function of Ω_m and σ_8 (in particular, models with smaller Ω_m predict infall ending at much higher redshift). Thus there is an urgent need for simulations of BCG growth using the concordance cosmology.

6.3 Are First-Ranked LRGs drawn from the Universal Luminosity Function?

BCG show a large luminosity gap; moreover, the dominance of the BCG is observed to be independent of redshift. Thus suggests that whatever mechanism created this dominance must have taken place at $z > 0.4$. Scenarios in which recent cannibalistic activity fueled the BCG growth (e.g. Hausman & Ostriker 1978) are unlikely. Poorer systems have more dominant BCGs, suggesting that the process that makes these galaxies unusually luminous is not related to the presence of BCGs in crowded rich cluster cores. Using 211 clusters of galaxies selected from SDSS photometry, Kim et al. (2002b) found that BCG with $M_{12} > 0.5$ `mag` showed strong alignment with their host clusters, while those with weaker dominance showed no tendency to align. (See also Fuller, West & Bridges (1999) for similar results for MKW/AWM groups.) Taken together, these observations support the scenario of Dubinsky (1998) – essentially a generic feature of the hierarchical structure formation paradigm with Gaussian initial conditions – whereby major mergers during galactic infall along filaments create the BCG at moderate ($z \sim 0.5 - 1.0$) redshifts. Statistical sampling may explain why poorer systems (which host an LRG) have more dominant brightest members. Alternatively, these systems are preferentially located within older structures, and are dynamically more mature. The BCGs at the confluence of these structures are further along the evolution sequence, making them more dominant. Nevertheless, it suggests that the properties of BCGs are intimately related to the assembly history of the local matter density. These findings, however, run contrary to the standard candle nature of the BCG metric luminosities (Sandage 1972; Gunn & Oke 1975; Postman & Lauer 1995), and argue against a BCG special population independent of local conditions. Properties of BCG clearly depend on environment and yet they are standard candles. We do not have a full understanding of this dichotomy.

7 CONCLUSIONS

We have shown that the luminosity gap, M_{12} between the first-ranked galaxy and the second-ranked in fields containing at least one LRG is large, and this is inconsistent with these brightest members being the statistical extreme of the local galaxy luminosity function within Scott (1957)'s model. This dominance of the brightest members changes little over the redshift range of $0.12 < z < 0.38$, and is more prominent in the poorer group-like LRG fields than the richer cluster-like fields. Furthermore, the brightest member in cluster-like LRG fields are systematically brighter (0.1–0.2 `mag`) in the mean than in group LRG fields. When we combine these findings with the conclusions of Kim et al. (2002b) and Fuller, West & Bridges (1999) that dominant brightest members are preferentially aligned with their host clusters, our results support the assembly of BCGs during cluster collapse within

the framework of hierarchical structure formation, and put stringent constraints on the growth of BCGs through recent accretion of lesser members. In future papers, we will present a statistical analysis of the optical environments of this volume-limited sample of LRG (Loh et al. 2005b), and their relationship with intermediate redshift clusters selected by X-ray emission (Loh et al. 2005c).

ACKNOWLEDGMENTS

We thank Rita Kim, Marc Postman, Tod Lauer, Jim Gunn, Scott Tremaine, Michael Blanton, David Hogg, Don Schneider, Tim Mckay, Richard Cool and Daniel Eisenstein for suggestions.

Funding for the creation and distribution of the SDSS Archive has been provided by the Alfred P. Sloan Foundation, the Participating Institutions, the National Aeronautics and Space Administration, the National Science Foundation, the U.S. Department of Energy, the Japanese Monbukagakusho, and the Max Planck Society. The SDSS Web site is `http://www.sdss.org/`.

The SDSS is managed by the Astrophysical Research Consortium (ARC) for the Participating Institutions. The Participating Institutions are The University of Chicago, Fermilab, the Institute for Advanced Study, the Japan Participation Group, The Johns Hopkins University, the Korean Scientist Group, Los Alamos National Laboratory, the Max-Planck-Institute for Astronomy (MPIA), the Max-Planck-Institute for Astrophysics (MPA), New Mexico State University, University of Pittsburgh, University of Portsmouth, Princeton University, the United States Naval Observatory, and the University of Washington. YSL and MAS acknowledge the support of NSF grant AST-0307409.

REFERENCES

Abazajian K. et al., 2003, AJ, 126, 2081
Abazajian K. et al., 2004, AJ, 128, 502
Abazajian K. et al., 2005, AJ, 129, 1755
Abell G.O., 1965, ARA&A, 3, 1
Albert C., White, R., Morgan, W., 1977, ApJ, 211, 309
Aragón-Salamanca A., Baugh C.M., Kauffmann G., 1998, MNRAS, 297, 427
Athanassoula E., Garijo A., Garca Gómez C., 2001, MNRAS, 321, 353
Bautz L.P., Morgan W.W., 1970, ApJL, 162, 149
Blakeslee J.P. et al., 2003, ApJL, 596, 143
Blanton M. et al., 2001, AJ, 121, 2358
Blanton M. et al., 2003a, ApJ, 592, 819
Blanton M. et al., 2003b, AJ, 125, 2276
Blanton M. et al., 2004, AJ, in press, astro-ph/0410166
Bhavsar S.P., Barrow J.D., 1985, MNRAS, 213, 857
Binney J., 1977, MNRAS, 181, 735
Bode P.W., et al., 1994, ApJ, 433, 479
Burke D.J., Collins C.A., Mann R.G., 2000, ApJL, 532, L105
Colless M., 1989, MNRAS, 237, 799
Cool R., et al., 2005, in press
Dalcanton J., 1998, ApJ, 495, 251
Djorgovski S., Davis M., 1987, ApJ, 313, 59
Dressler A., 1978, ApJ, 222, 23
Dressler A., Gunn J.E., 1983, ApJ, 270, 7
Dressler A. et al., 1987, ApJ, 313, 42
Dubinsky J., 1998, ApJ, 502, 141
Eddington A.S., 1913, MNRAS, 73, 359
Ellis R.S. et al., 1997, ApJ, 483, 582
Eisenstein D.J. et al., 2001, AJ, 122, 2267
Eisenstein D.J. et al., 2003, ApJ, 585, 694
Eisenstein D.J. et al., 2005, ApJ, 619, 178
Fukugita M., Ichikawa T., Gunn J.E., Doi M., Shimasaku K., Schneider D.P., 1996, AJ, 111, 1748
Fuller T.M., West M.J., Bridges T.J., 1999, ApJ, 519, 22
Fioc M., Rocca-Volmerange B., 1997, A&A, 326, 950
Gao L. et al., 2004, 614, 17
Garilli B., Maccagni D., Andreon S., 1999, A&A, 342, 408
Geller M., Peebles P.J.E., 1976, ApJ, 206, 939
Geller M., Postman M., 1983, ApJ, 274, 31
Goto T. et al., 2003, PASJ, 54, 515
Graham A. et al., 1996, ApJ, 465, 534
Gunn J.E., Oke J.B., 1975, ApJ, 195, 255
Gunn J.E., Tinsley B.E., 1977, ApJ, 210, 1
Gunn J.E. et al., 2003, AJ, 116, 3040
Hausman M.A., Ostriker J.P., 1978, ApJ, 224, 320
Hoessel J.G., Gunn J.E., Thuan T.X., 1980, ApJ, 241, 486
Hogg D.W., Finkbeiner D.P., Schlegel D.J., Gunn J.E., 2001, AJ, 122, 2129
Hubble E., 1936, ApJ, 84, 158
Hunsberger S.D., Charlton J.C., Zaritsky, D., 1998, ApJ, 505, 536
Ivezic Z. et al., 2004, AN, 325, 583
Jones L.R., Ponman T.J., Forbes D.A., 2000, MNRAS, 312, 139
Jones L.R. et al., 2003, MNRAS, 343, 627
Stuart A., Ord J.K., 1987, *Kendall's Advanced Theory of Statistics, Vol. 1:Distribution Theory*, $5^{\rm th}$ Edition, Arnold Publishers
Kiang T., 1961, MNRAS, 122, 263
Kim R.S.J. et al., 2002a, AJ, 123, 20
Kim R.S.J. et al., 2002b, ASP Conf. Ser., 268, 393
Lawless J.F., 1982, *Statistical Models and Methods for Lifetime Data*, John Wiley & Sons
Lawrence A. et al., 1986, MNRAS, 219, 687
Lauer T.R., Postman M., 1994, ApJ, 425, 418
Loh Y.S., 2003, Ph.D Thesis, Princeton University
Loh Y.S., Strauss M.A. et al., 2005a, in prep.
Loh Y.S., Strauss M.A. et al., 2005b, in prep.
Loh Y.S. et al., 2005c, in prep.
Loveday J. et al.,1992, ApJ, 390, 338
Lubin L.M., 1996, AJ, 112, 23
Lugger P.M., 1989, ApJ, 343, 572
Lumsden S.L. et al., 1997, MNRAS, 290, 119
Lupton R.H. et al., 2001, ASP Conf. Ser., 10, 269
Merritt D., 1984, ApJ, 276, 26
Merritt D., 1985, ApJ, 289, 18
Morgan W. W., Kayser S., White R. A., 1975, ApJ, 199, 545
Mulchaey J.S., Zabludoff, A.I., 1999, ApJ, 514, 133
Mulchaey J.S., 2000, ARAA, 38, 289
Nipoti C. et al., 2003, MNRAS, 344, 748
Norberg P. et al., 2002, MNRAS, 332, 827
Oegerle W.R., Hoessel J.G., ApJ, 375, 15
Ostriker J.P., Tremaine S.D., 1975, ApJ, 202, 113
Ostriker J.P., Hausman M.A., 1977, ApJ, 217, 125
Padmanabhan N. et al., 2004, astro-ph/0407594
Paolillo M. et al., 2001, A&A, 367, 59
Petrosian V., 1976, ApJL, 209, L1
Peterson B.A., 1970, ApJ, 159, 333
Peebles P.J.E., 1968, ApJ, 153, 13
Pier J.R. et al., 2003, AJ, 125, 1559
Ponman T.J. et al., 1994, Nature, 369, 462
Postman M., Lauer T.R., 1995, ApJ, 440, 28

Press W.H., Schechter P.L., 1974, ApJ, 187, 425
Rees M.J., Ostriker J.P., 1977, MNRAS, 179, 541
Richstone D.O., 1975, ApJ, 200, 535
Richstone D.O., 1976, ApJ, 204, 642
Sandage A., 1972, ApJ, 178, 1
Sandage A., Hardy E., 1973, ApJ, 183, 743
Schechter P.L., 1976, ApJ, 203, 297
Schechter P.L., Peebles P.J.E., 1976, ApJ, 209, 670
Schechter P.L., 2002, in *Lighthouses of the Universe: The Most Luminous Celestial Objects and Their Use for Cosmology*, (eds. Sunyaev et al.), ESO Astrophysics Symposia, Springer Verlag
Schlegel D.J., Finkbeiner D.P., Davis M., 1998, ApJ, 500, 525
Schmidt M, 1968, ApJ, 151, 393
Schneider D.P., Gunn J.E., Hoessel J.G., 1983, ApJ, 264, 337
Scott E., 1957, AJ, 62, 248
Scranton R. et al. 2002, ApJ, 579, 48
Smith J.A. et al., 2002, AJ, 123, 2121
Stanford S.A., Eisenhardt P.R., Dickinson M., 1998, ApJ, 492, 461
Stoughton C. et al., 2002, AJ, 123, 485
Strauss M.A. et al., 2002, AJ, 124, 1810
Tegmark M. et al., 2004, ApJ, 606, 702
Tremaine S., Richstone D., 1977, ApJ
Tremaine S., 1990 in *Dynamics and Interaction of Galaxies*, (ed. Wielen, R.), Springer Verlag
Trentham N., 1998, MNRAS, 294, 193
Valotto C.A. et al., 1997, ApJ, 479, 90
van Dokkum P.G. et al., 1998, ApJ, 504, L17
West J.M., 1994, MNRAS, 268, 79
White S.D.M., 1976, MNRAS, 177, 717
Yagi M. et al., 2002, AJ, 123, 87
York D. et al., 2000, AJ, 120, 1579

APPENDIX A: A CONSISTENT POPULATION OF LRG

As discussed earlier in the main text and in Eisenstein et al. (2001), the LRG target selection will only give a consistent population for $z > 0.23$. In particular, for $r < 17.5$, the selection admits many intrinsically fainter galaxies. Furthermore, bright galaxies are at the exponential tail of the luminosity function, and small deviations from the nominal LRG luminosity threshold affect the derived number counts substantially. Since the flux-limited MAIN galaxy survey is spectroscopically complete to $r \sim 17.8$ or $M^* - 1$ at $z \sim 0.25$, we spectroscopically trimmed the low redshift LRG to match the rest-frame color and luminosity of their higher redshift counterparts. We use the empirically derived color-redshift relation of $M^* - 1$ red sequence galaxies from Appendix B to extract a co-evolving population of similar color and luminosity.

Figure A1 shows plots of the color-magnitude relation for galaxies from the SDSS MAIN galaxy survey. The color used is $c_{\rm LRG} = 7/9g + 5/3r - 4i$, which is approximately parallel to the color locus of LRGs; see Figure B1. The figure shows three narrow redshift slices ($\Delta z = 0.01$) at $z = 0.10, 0.15$, and 0.20. The red sequence is clearly visible. The axes for the first three panels (both top and bottom left) are labeled in *observed* quantities, but shifted relative to the red sequence for direct comparison between the redshift subsamples. The fourth panel (bottom right) is a combined plot of the three, where the axis is now labeled in rest-frame quantities. We employ a single model *k+e* correction of a passively evolving early-type M^* galaxy from PEGASE to realign the $r_{\rm petro}$-axis for rest-frame comparison. Galaxies that pass the LRG target selection are indicated by violet points. The steep oblique selection edge is the color-luminosity bound that imposed a red bias to LRGs. Notice that the selection is more permissive at $z = 0.1$, but becomes gradually more stringent at $z \approx 0.2$[4]. At $z = 0.1$ (top left panel), a $\sim M^* - 0.5$ galaxy with the exact red-sequence color (i.e. one that lies on the solid line) would pass the LRG target selection (and be colored violet), but at $z = 0.2$ (bottom left), it would have to have an absolute magnitude $\sim M^* - 1$ to make the cut. The red box is the proposed rest-frame color-luminosity cut. When applied uniformly across cosmological epoch, we obtained a trimmed sample of consistent LRG population with a roughly constant comoving density (cf. Figure 1). The slight increase in density at higher redshift is not real but a consequence of Eddington bias from larger photometric uncertainties at high redshift.

APPENDIX B: EMPIRICAL COLOR-REDSHIFT RELATION

Since galaxies are clustered, their neighbors tend to be at the same redshift. Hence, by using a set of reference galaxies (LRG or QSO) with spectroscopic redshifts, one can infer the average *unbiased* color (and other photometric attributes) of a typical galaxy at those redshifts from the properties of galaxies that clustered around these reference galaxies, even though the selection of the original reference galaxies maybe biased. Specifically, for spectra obtained with the SDSS, while both LRGs and QSOs are color selected, and thus by design have a biased mean color, the more numerous galaxies from the deeper imaging data that cluster around these spectroscopic objects are not. By stacking fields of LRGs or QSOs with similar redshifts to make a composite galaxy field at those redshifts, background and foreground galaxies seen in projection can be removed statistically as they are not expected to correlate with the reference spectra.

We have calibrated the color-redshift relation and the *observed* scatter, in two color dimensions ($g - r$ and $r - i$) for galaxies with a fixed absolute magnitude range ($M^* - 2.5 < r_{\rm petro} < M^*$). An evolving model of an old stellar population elliptical galaxies from PEGASE (Fioc & Rocca-Volmerange 1997) was used to compute the r-band magnitude for a M^* galaxy as a function of redshift. Two luminosity ranges were computed: (1) using $M^* - 2.5 < r_{\rm petro} < M^* - 0.8$ for $\sim M^* - 1$ LRG-like galaxies, (2) $M^* - 1.5 < r_{\rm petro} < M^* + 0.5$ for $\sim M^*$ red sequence galaxies. We employ an optimal weighting using a two dimensional elliptical Gaussian to locate the peak and estimate the scatter of the locus. Details on how this is done and measurements of *intrinsic* scatter of the red sequence to constrain the spread of formation time scale of old stars as a function of redshift, as well as comparison between colors of galaxies in the neighborhood of LRGs and QSOs will be discussed in a subsequent paper (Loh et al. 2005a).

Figure B1 is the $g - r$ and $r - i$ color-color diagram of red-sequence galaxies with $r_{\rm petro} \approx M^*$. The solid ellipses are the

[4] As an interesting aside, notice that even though the LRG target selection is permissive at $z \approx 0.10$, it still primarily selects galaxies on the red-sequence, as contamination from blue star-forming galaxies is minimal. Thus one could in principle cleanly extend the LRG selection of red galaxies to ~ 0.8 `mag` lower luminosity, increasing the LRG comoving number density by a factor ~ 3 (Padmanabhan et al. 2004)

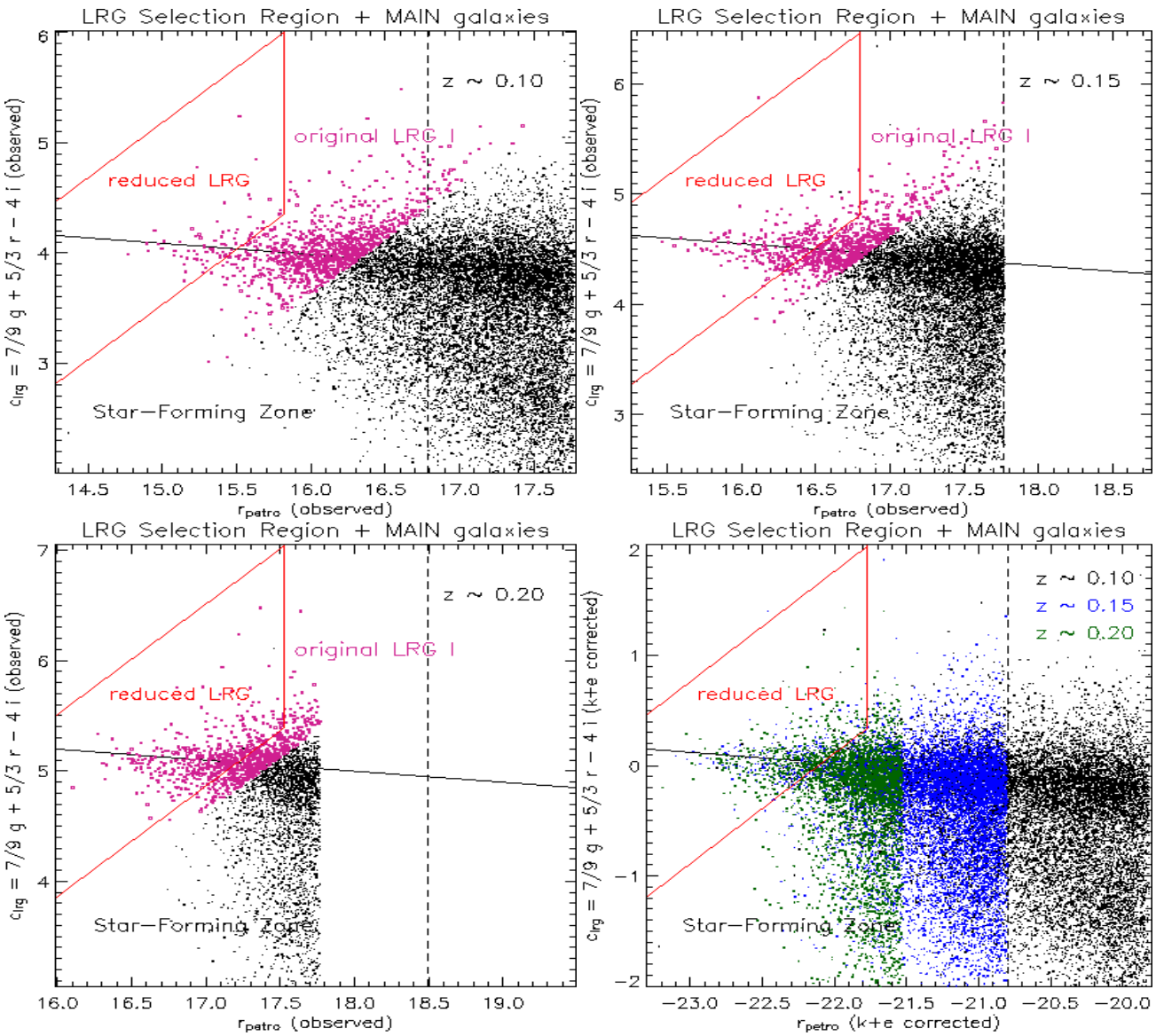

Figure A1. These panels show the observed color magnitude diagrams of LRG and MAIN sample galaxies in three redshift ranges. The axes for the two top and the bottom left panels are in observed quantities. A model *k+e* correction for an old stellar population sequence is used to shift the x-axes to the same luminosity range. M^* at the respective redshifts of (0.1, 0.15, 0.2 ($\Delta z = 0.01$)) of the panels are aligned, and is indicated by the dashed vertical line. The location of the red sequence – the sloping horizontal line – for a fixed absolute magnitude is used to shift the y-axis to the same rest-frame color. The diagrams are made using spectroscopic galaxies brighter than $r_{\rm petro} \sim 17.8$ from the MAIN sample. Hence, they are unbiased with respect to color. The violet points are these MAIN galaxies that also pass the LRG Cut I selection criteria. The red box is the rest-frame color-magnitude cut used here for the consistent trimmed LRG sample. The last panel (bottom right) plots all galaxies from the other three panels, now shown in rest-frame quantities.

1σ contours while the gray ellipses are 3σ. The locus of early type galaxy follows an approximate linear sequence with redshift up to the up-turn point at around $z \approx 0.37$, motivating the "Cut I" of the LRG target selection (Eisenstein et al. 2001). There is a slight kink at $z \approx 0.26$, which corresponds to the M star locus crossing with this early-type locus. The analysis was done using $\sim 30,000$ LRG and QSO in the redshift range of $0.08 < z < 0.44$ and 2340 deg^2 of DR1 imaging data processed with `photo` 5.3 photometry.

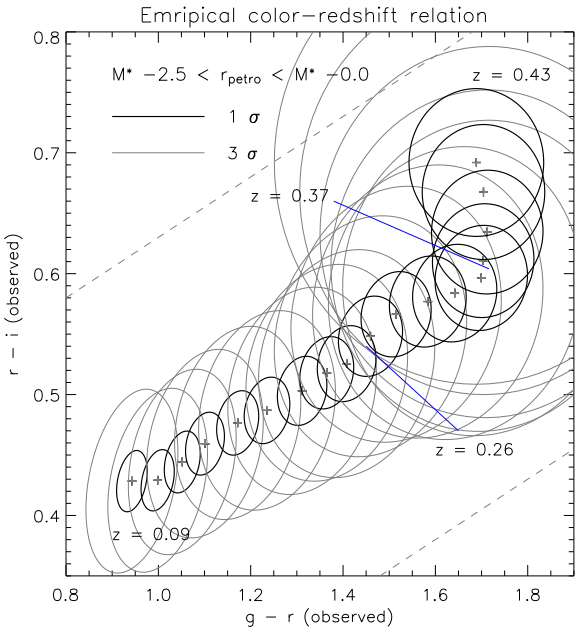

Figure B1. The empirically determined locus of red sequence M^* galaxies from $z = 0.09$ to $z = 0.43$ in increments of $\Delta z = 0.02$. The ellipses in black (grey) are the $1\,(3)\,\sigma$ dispersion of colors at each redshift. This sequence of ellipses serves as a pseudo photometric redshift filter to reduce contamination from background galaxies.